Non-invasive Activation Times Estimation Using 3D Echocardiography

Adityo Prakosa[1], Maxime Sermesant[1], Hervé Delingette[1], Eric Saloux[2], Pascal Allain[3], Pascal Cathier[3], Patrick Etyngier[3], Nicolas Villain[3], and Nicholas Ayache[1]

[1] Asclepios Research Project, INRIA Sophia-Antipolis, France
[2] Service de Cardiologie CHU Caen, France
[3] Medisys, Philips Healthcare Suresnes, France

Abstract. Despite advances in both medical image analysis and intracardiac electrophysiological mapping technology, the understanding of cardiac mechano-electrical coupling is still incomplete. This knowledge is of high interest since it would help estimating the cardiac electrophysiology function from the analysis of widely available cardiac images, such as 3D echocardiography. This is important, for example, in the evaluation of the cardiac resynchronization therapy (CRT) where the placement and tuning of the pacemaker leads plays a crucial role in the outcome of the therapy. This paper proposes a method to estimate activation times of myocardium using a cardiac electromechanical model. We use Kernel Ridge Regression to find the relationship between the kinematic descriptors (strain and displacement) and the contraction force caused by the action potential propagation. This regression model is then applied to two 3D echocardiographic sequences from a patient, one in sinus rhythm and the other one with left ventricle pacing, for which strains and displacements have been estimated using incompressible diffeomorphic demons for non-rigid registration.

Keywords: cardiac electrical mapping, Kernel Ridge Regression, 3D echocardiography.

1 Introduction

The wide availability of cardiac imaging modalities especially 3D echocardiography allows clinicians to estimate some geometrical characteristics of the myocardium motion such as displacement, strain or strain rate. However, these quantities are only related to the kinematics of the heart whereas in many cases it is important to also obtain information about the patient's cardiac electrical propagation. Indeed contact or non-contact intracardiac electrical mappings are invasive procedures which are not classically used for diagnosis but rather for applying a therapy. Electrocardiographic imaging[1] (*a.k.a.* body surface potential mapping) is a non-invasive technique for imaging activation times of the myocardium but still remains to be validated thoroughly and is not widely available in clinical centers. Therefore there is a strong need to quantitatively assess a

O. Camara et al. (Eds.): STACOM-CESC 2010, LNCS 6364, pp. 212–221, 2010.

patient electrophysiological condition from non-invasive imaging modalities such as 3D echocardiography. This is especially valid in the context of cardiac resynchronization therapy (CRT) for which up to 30% of the patients with pacemaker leads show no benefit[2]. Providing activation maps from a 3D echocardiography for instance, would be of great interest to select patients responding to the therapy and to optimize the lead placements and delays during and after therapy. More fundamentally, understanding the relationship between cardiac mechanics and electrophysiology is essential to improve the diagnosis and therapy of patients suffering from heart failure.

A study on the relation between cardiac magnetic resonance (MR) motion tracking and the electrical activation pattern has been published by Sanchez-Ortiz *et al.*[3] which combines some cardiac motion descriptors in order to obtain the electrical activation time. However, in this study, the weights were assigned manually to get an estimation of the activation. McVeigh *et al.*[4] also consider only the circumferential strain estimated from tagged MR images as the mechanical activation measure. Very high frame rate ultrasound in electromechanical imaging (EWI), which could map the electromechanical wave (EMW) correlated with cardiac electrical activation in 2D echocardiography, has been published by Provost *et al.*[5]. However, understanding the 3D cardiac electrical propagation is still very important for clinicians.

In this paper, our main objective is to find a relationship between the different kinematic parameters obtained from cardiac image analysis and the activation times of the myocardium using a machine learning method. The activation times are defined as moments at which the activation forces at a given point sharply increase. Activation times are strongly correlated with the action potential signal through the mechano-electrical coupling.

The training stage is based on motion and contraction forces estimated from an electromechanical model of the heart. This *in silico* cardiac model serves as a reference model in the absence of reliable intracardiac mapping information. Several pathologies and pacing scenarios are considered in this training phase. Based on this learning process, we can predict the cardiac electrical propagation from kinematic parameters estimated from cardiac image analysis. This approach has been evaluated on synthetic cases as well as on one patient. The results are thoroughly discussed and perspectives of this work are provided in a final section.

2 3D Echocardiography Image Registration and Motion Estimation

We use 3D echocardiography images provided by the University Hospital of Caen, Normandy - France. This data was acquired from patients under CRT with two implanted electrodes, one in the left ventricle and the other in the right ventricle. Two different pacemaker stimulation modes were imaged and analysed. The first mode corresponds to the sinus rhythm mode when no pacemaker lead is activated. In the second mode, the left ventricle is stimulated. Left ventricle segmentation along whole cardiac sequence was provided by the Medisys Group

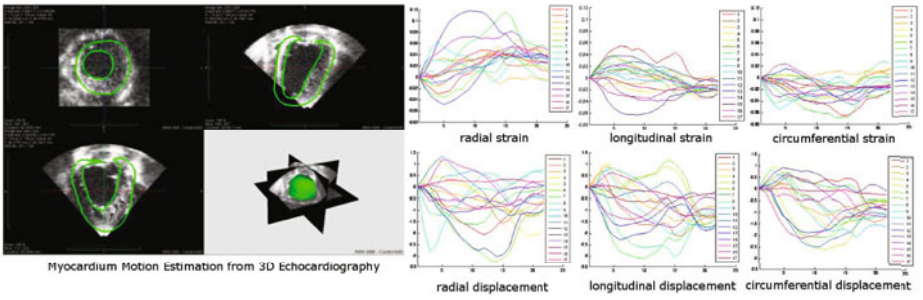

Fig. 1. 3D echocardiography myocardium motion estimation. Myocardium motion is tracked and then strains and displacements with respect to the first reference image in the cardiac cycle are computed and projected in a local frame representing the radial, longitudinal and circumferential directions. The different colors in the curves show the 17 different AHA zones. The strain and displacement curves shown are from a patient with LBBB and without any pacemaker stimulation. The strain vertical axis is dimensionless while the displacement vertical axis is in millimeters. The horizontal axis shows the image frame number in the cardiac cycle.

of Philips Healthcare, Suresnes - France. The 3D echocardiography sequence begins at the end-diastolic phase of the cardiac cycle.

2.1 Incompressible Diffeomorphic Demons

Cardiac motion is estimated through a non-linear image registration algorithm applied between consecutive frames of the same cardiac cycle. The purpose of applying this non-linear image registration is to find the displacement vector field $\mathbf{u(x)}$ associated with the transformation $\phi(\mathbf{x}) = \mathbf{x} + \mathbf{u(x)}$ which aligns a template image $\mathrm{T}(\mathbf{x})$ to a reference image $\mathrm{R}(\mathbf{x})$, where $\mathbf{x} \in \mathbb{R}^3$ is the space coordinate (voxel (x,y,z)). This displacement vector field $\mathbf{u(x)}$ is considered as the cardiac displacement field. All images in the cardiac sequence are registered to the same reference image which is the first image of the 3D echocardiography sequence, corresponding to the end-diastolic phase.

We take into account the myocardium near-incompressibility assumption (maximum 5 to 7% of volume variation during the cardiac cycle) by relying on the incompressible demons algorithm proposed by Mansi *et al.*[6] to estimate cardiac motion. This algorithm improves the diffeomorphic demons algorithm[7] by adding 2 constraints: the myocardium near-incompressibility and linear elastic regularization of velocity fields. This method has been developed and evaluated for cardiac motion estimation on cine MRI images [6].

A 3D myocardium segmentation for the first frame of the sequence is used as the incompressible region. The 3D echocardiography sequence starts at the end-diastolic phase of a cardiac cycle. All image frames in the 3D echocardiography sequence are being registered to this end-diastolic frame.

The recovered displacement vector field is projected in the radial, circumferential and longitudinal directions using the heart local coordinate system.

2.2 Strain Estimation

The displacement vector field $\mathbf{u(x)}$ which recovers the cardiac motion $\phi(\mathbf{x}) = \mathbf{x}+\mathbf{u(x)}$ is then used to compute the Lagrangian finite strain tensor $E = \frac{1}{2}(\nabla\mathbf{u}+\nabla\mathbf{u}^T+\nabla\mathbf{u}^T\nabla\mathbf{u})$. The strain is calculated by using the end-diastolic frame as the reference image $\mathrm{R}(\mathbf{x})$. Similarly for the displacement vector field, the obtained strain is projected in the radial, circumferential and longitudinal directions (cf. Fig. 1).

3 Inverse Mechano-Electrical Coupling

3.1 Electromechanical Model

In order to learn how the cardiac kinematics are related to the cardiac electrophysiology it is necessary to get for the same patient descriptors of the cardiac motion and electrical wave propagation. This could be provided by 3D echocardiography and intracardiac electrophysiological mapping acquired on the same patient. To merge both information, the patient must be in the same stimulation mode and endocardial surfaces reconstructed from intracardiac mappings must match those segmented in 3D US. However, such joint acquisition was not available in our study. Therefore, we proposed to use an electromechanical model of the heart [8] to simulate patient cases. From those simulated cases, we could obtain both electrophysiological and kinematic measurements. To be realistic, this model uses the cardiac anatomy extracted from echocardiography images as a priori information about the shape of the left ventricle (LV). We simulated four cardiac cases using the electromechanical model to create a training database. First, we simulate the cardiac propagation and contraction in normal sinus rhythm where the electrical simulation is coming from the left and right ventricle endocardium. In the second simulation, we simulate a left bundle branch block (LBBB) where the stimulation is coming only from the right ventricle endocardium while the third simulation is the right bundle branch block (RBBB) case where stimulation is coming only from the left ventricle endocardium. The last case is the bi-ventricular pacing case where we initiate the electrical propagation from a zone in the lateral freewall and a zone in the right ventricle apex in order to simulate the pacemaker bi-ventricular pacing (cf. Fig. 2).

The simulation gives the deformation of the cardiac mesh along with the contraction value and the potential value for each point in the mesh. We perform a thresholding in order to obtain the time at which the contraction value increases. We also compute the displacement vector field which maps the myocardium at a given time point to the end-diastolic image of the sequence. Kinematic descriptors extracted from the obtained displacement vector field are the displacement and the strain projected in the radial, longitudinal and circumferential directions.

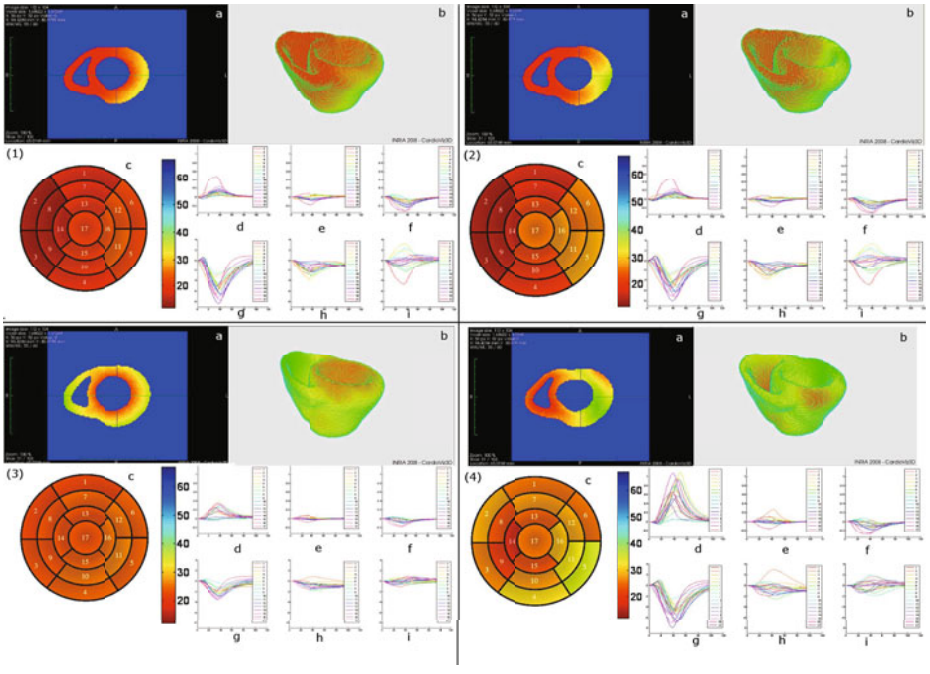

Fig. 2. Electromechanical simulation. 4 cardiac cases simulated using the electromechanical model. (1) normal case, (2) LBBB case, (3) RBBB case and (4) biventricular pacing case. (a), (b) and (c) are the contraction force isochrone. (c) is the isochrone for the LV divided to 17 AHA zones. (d), (e), (f) are the radial, longitudinal and circumferential strains respectively and (g), (h), (i) are the radial, longitudinal and circumferential displacements. Axis units are as explained in Fig. 1. These strains and displacements are extracted from the deformation of the mesh simulated by the electromechanical model.

3.2 Kernel Ridge Regression as a Learning Method

Using an electromechanical model of the heart, we learn the relationship between the kinematic descriptors and the electrical activation. We use Kernel Ridge Regression to find a relationship between these 2 quantities.

Ridge Regression searches a linear function $\mathbf{y} = \mathbf{w}^T\mathbf{x}$ that models the dependencies between the descriptor vectors $\mathbf{x}_i \in \mathbb{R}^d$ and the response vectors $\mathbf{y}_i \in \mathbb{R}^r$ (all vectors are column vectors) from a set of T examples $(\mathbf{x}_1, \mathbf{y}_1), (\mathbf{x}_2, \mathbf{y}_2), ..., (\mathbf{x}_T, \mathbf{y}_T)$. Classically, we need to minimize the quadratic cost $C(\mathbf{w}) = \frac{1}{2}\sum_i^T (\mathbf{y}_i - \mathbf{w}^T\mathbf{x}_i)^2$, where $\mathbf{w}$ is a $d \times r$ matrix. Regularizing this equation, the total cost function which needs to be minimized hence becomes $C(\mathbf{w}) = \frac{1}{2}\sum_i^T (\mathbf{y}_i - \mathbf{w}^T\mathbf{x}_i)^2 + \frac{1}{2}\lambda \|\mathbf{w}\|^2$, where $\lambda > 0$ is the regularization parameter. Introducing a $T \times d$ matrix $X = (\mathbf{x}_1, \mathbf{x}_2, ..., \mathbf{x}_T)^T$ which contains the vectors $\mathbf{x}_i$ in its row and a $T \times r$ matrix $Y = (y_1, y_2, ..., y_T)^T$ which contains the vectors $\mathbf{y}_i$ in its row, the equation can be written as $C(\mathbf{w}) = \frac{1}{2}\|Y - X\mathbf{w}\|^2 + \frac{1}{2}\lambda\|\mathbf{w}\|^2$.

Minimizing this function by taking its derivative with respect to $\mathbf{w}$ and setting it equal to zero gives $-X^TY + X^TX\mathbf{w} + \lambda\mathbf{w} = 0 \Rightarrow \mathbf{w} = \left(\lambda\mathbf{I} + X^TX\right)^{-1} X^TY$.

Ridge Regression can be extended to Kernel Ridge Regression by rewriting the solution $\mathbf{y} = \mathbf{w}^T\mathbf{x} = \left(\left(\lambda\mathbf{I} + X^TX\right)^{-1} X^TY\right)^T \mathbf{x} = Y^T\left(\lambda\mathbf{I} + XX^T\right)^{-1} X\mathbf{x} = Y^T\left(\lambda\mathbf{I} + K\right)^{-1}\mathbf{k}$ with $K = XX^T$ and $\mathbf{k} = X\mathbf{x}$. We choose to use Radial Basis Function as a Kernel function $K(x_i, x_j) = e^{-\frac{|x_i - x_j|}{\sigma^2}}$ with $i, j = \{1, ..., T\}$.

Parameter Optimization. The chosen λ and σ parameters are optimized by using leave-one-out estimates which train the model with all members of the training set but one and test the performance on the singleton. The process is repeated for all the singletons in the training set. We use Allen's PRESS (predicted residual sum of squares) statistic for this process, $PRESS = \sum_i^T \mathbf{e}_{(i)}^2$ [9], where $\mathbf{e}_{(i)} = \mathbf{y}_i - \hat{\mathbf{y}}_{(i)}$ is the residual for the ith example with the ith example excluded from the training process and $\hat{\mathbf{y}}_{(i)}$ is the predicted response for the ith example based on the training process. Fortunately, we have $e_{(i)} = \frac{e_i}{1-h_{ii}}$ where $e_i = \mathbf{y}_i - \hat{\mathbf{y}}_i$ is the residual for the ith example in the training process which includes all examples and $\hat{\mathbf{y}}_i$ is the fitted response based on this training. h_{ii} is the ith element of the leading diagonal of the hat matrix $H = X(\lambda\mathbf{I} + X^TX)^{-1}X^T = XX^T(\lambda\mathbf{I} + XX^T) = K(\lambda\mathbf{I} + K)^{-1}$. Therefore, in the end, we can have the PRESS for the chosen parameters λ and σ in one iteration. We use the downhill simplex search method in MATLAB in order to optimize these parameters to have the smallest PRESS.

With this approach, we learn a non-linear relationship (due to the choice of Radial Basis Function as the Kernel function) between the kinematic descriptors and the activation force caused by the action potential. We take the radial, longitudinal and circumferential strains ($\mathbf{E}_r, \mathbf{E}_l, \mathbf{E}_c \in \mathbb{R}^{t_d}$) and also the radial, longitudinal and circumferential displacements ($\mathbf{u}_r, \mathbf{u}_l, \mathbf{u}_c \in \mathbb{R}^{t_d}$) from points in the myocardium as the components of the kinematic descriptor vector $\mathbf{x}_i \in \mathbb{R}^{d=6\times t_d}$, where t_d is the number of each descriptor sampling time in a cardiac sequence. The contraction force along a cardiac cycle t_r is set as the response vector $\mathbf{y}_i \in \mathbb{R}^{r=t_r}$. The descriptor sampling time t_d is taken for 20 time instances in order to follow the temporal resolution of the real patient data. However, the response vector sampling time t_r is chosen as 100 time instances in order to have high temporal resolution of the contraction force along a cardiac cycle, starting before the beginning of the P wave of the ECG. The examples in the training set consist of the different points in the myocardium. We take 30 points from each of the American Heart Association (AHA) 17 zones so we have 510 learning points along a cardiac cycle. We separate the value σ for the displacement and the strain used in the Kernel $K(x_i, x_j) = e^{-\frac{|u_i - u_j|}{\sigma_u^2} - \frac{|E_i - E_j|}{\sigma_E^2}}$. Once the learning process is done, we obtain the optimal values for λ, σ_u and σ_E. We use these parameters to predict the other points in the myocardium in order to obtain the cardiac contraction force mapping caused by the potential.

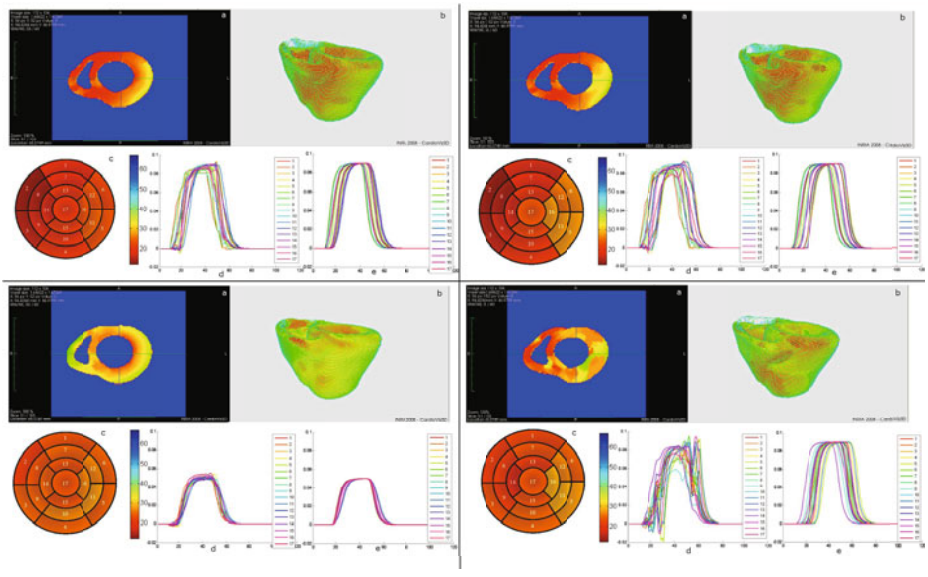

Fig. 3. Prediction of contraction forces from synthetic data. (a), (b) are the whole contraction force isochrones (activation times) obtained after applying the learning method on the whole points in the myocardium for case (1) (sinus rhythm), (2) (LBBB), (3) (RBBB) and (4) (bi-ventricular pacing) whereas (c) is the whole contraction force isochrone only for the left ventricle. (d) is the contraction force curve along a cardiac cycle which predicted by the learning method whereas (e) is the ground truth contraction force curve as produced by the electromechanical model. The vertical axis unit is in MPa. The horizontal axis shows the frame number in the cardiac cycle.

4 Results

4.1 Evaluation on Simulated Data

First, we tested our machine learning method using the simulated motion from the electromechanical model for which we have a ground truth to compare to. The first 3 cases which have been described in section 3.1 are included in our training set, whereas the fourth case has not been included. The optimal parameters of the regression have been found as $\lambda = 0.0004$, $\sigma_u = 107.1030$ and $\sigma_E = 9.0276$ which yield the root mean squared error (RMSE) value between the predicted and the ground truth value 0.0016 MPa. This seems to imply that strains are more correlated with activation times than displacements since their variances are smaller (for a similar range of values). We applied the regression method to all points of the first, second and third cases producing quite smooth predicted contraction force curves (see Fig. 3). Note that the training stage only included a very small subset of those points thus showing that the kernel ridge regression is able to generalize the correlations between strains and forces to the whole myocardium.

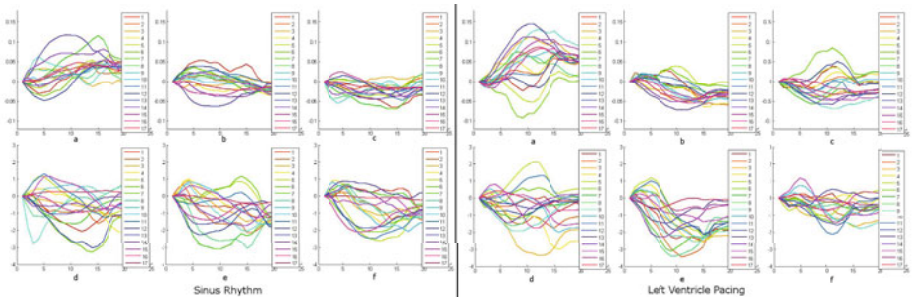

Fig. 4. Kinematic descriptors extracted from patient's 3D echocardiography. (a) (b) and (c) are the radial, circumferential and longitudinal strains whereas (d), (e) and (f) are the radial, circumferential and longitudinal displacements. Axis units are as explained in Fig. 1.

In the fourth case, the predicted force values are not as smooth as expected. However the predicted and the ground truth value of the fourth case have the same global bell shape where up and down slopes can be detected using thresholding. The bull's eyes plot computed from the estimated activation times also correspond to their expected value. In the second case (LBBB) we clearly have an early activation from the septal wall whereas in the third case (RBBB) the early activation originated from the endocardial wall of the left ventricle. In the fourth case (bi-ventricular pacing), not included in the training set, the delays between right and left ventricles are slightly decreased. The left ventricle RMSE value between the predicted and the ground truth activation time is 7 ms for the first 3 cases and 37 ms for the fourth case.

4.2 Application to Clinical Data

From the time series of 3D echocardiography images, we segmented the myocardium and then estimated the cardiac motion using the incompressible demons algorithm. The myocardium segmentation is used to specify the region where the incompressibility constraint must be satisfied. From the knowledge of the left ventricle axis, we can define the 3 local directions and then project strain tensors and displacements along those three directions (cf. Fig. 4). These values are then used as input descriptors in the regression method.

5 Discussion

The estimation of contraction forces for each AHA segment and for the two simulation modes are shown in Fig. 5. The estimated curves of contraction forces are noisy as in the case of simulated data but also no longer have a bell shape. In particular, those curves have negative parts at the beginning of systole whereas

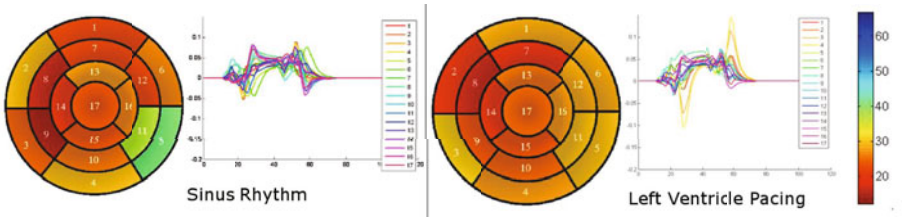

Fig. 5. Patient contraction force prediction. Predicted contraction force time and activation time isochrone (bull's eyes) for two different pacemaker stimulation mode from the same patient. Axis units are as explained in Fig. 3.

they have been trained to be positive. Those curves have been thresholded (value chosen as 0.03) to obtain two bull's eyes plot of activation times for the sinus rhythm and left ventricular pacing. It should be noticed that the late activation in green on the lateral wall of the left ventricle at sinus rhythm has been activated much earlier after pacing in the left ventricle which is expected.

From the preliminary results obtained on one patient with 2 stimulation modes, the estimation of activation times seems to correspond to the expected values. However, the shape and negative values of the estimated contraction forces indicate that the regression model does not capture well the observations. This may originate from several factors. First of all, there may be a difference of patterns between the simulated strains and displacement and the ones estimated by the non-linear registration. Second, there is a slight error when choosing the reference end diastolic image which produces significant errors in the estimation of strains. One could cope with those errors by having several regression methods corresponding to several choices of reference images. Finally, it should be noted that the electromechanical model involved for training the method used the anatomy of the left ventricle of the patient (see section 3.1) on which it was evaluated. Further evaluation on more patient images should indicate whether the learning method is sensitive to the patient anatomy.

6 Conclusion

We presented in this paper a method to estimate contraction forces and activation times from echocardiographic images. A supervised learning method has been proposed which relies on synthetic measurements from an electromechanical model of the heart for the training stage. The method has been evaluated on synthetic data and a patient case. Further work will test the proposed method on a larger sets of patients with various stimulation protocols. Sensitivity of our approach to the estimation of strains and the choice of the reference image will be studied. Learning from intracardiac electrophysiological mapping and 3D echocardiography of the same patient should improve the result and will be done as soon as the data is acquired.

References

1. Ghanem, R.N., Jia, P., Ramanathan, C., Ryu, K., Markowitz, A., Rudy, Y.: Noninvasive electrocardiographic imaging (ECGI): comparison to intraoperative mapping in patients. Heart Rhythm 2, 339–354 (2005)
2. Helm, R.H., Byrne, M., Helm, P.A., Daya, S.K., Osman, N.F., Tunin, R., Halperin, H.R., Berger, R.D., Kass, D.A., Lardo, A.C.: Three-dimensional mapping of optimal left ventricular pacing site for cardiac resynchronization. Circulation 115, 953–961 (2007)
3. Sanchez-Ortiz, G., Sermesant, M., Chandrashekara, R., Rhode, K., Razavi, R., Hill, D., Rueckert, D.: Detecting the onset of myocardial contraction for establishing inverse electro-mechanical coupling in xmr guided rf ablation. In: Proceedings of IEEE International Symposium on Biomedical Imaging, Arlington, USA, pp. 1055–1058 (2004)
4. McVeigh, E.R., Prinzen, F.W., Wyman, B.T., Tsitlik, J.E., Halperin, H.R., Hunter, W.C.: Imaging asynchronous mechanical activation of the paced heart with tagged MRI. Magn. Reson. Med. 39, 507–513 (1998)
5. Provost, J., Lee, W.N., Fujikura, K., Konofagou, E.E.: Electromechanical wave imaging of normal and ischemic hearts in vivo. IEEE Trans. Med. Imaging 29, 625–635 (2010)
6. Mansi, T., Peyrat, J.M., Sermesant, M., Delingette, H., Blanc, J., Boudjemline, Y., Ayache, N.: Physically-constrained diffeomorphic demons for the estimation of 3d myocardium strain from cine-MRI. In: Ayache, N., Delingette, H., Sermesant, M. (eds.) FIMH 2009. LNCS, vol. 5528, pp. 201–210. Springer, Heidelberg (2009)
7. Vercauteren, T., Pennec, X., Perchant, A., Ayache, N.: Non-parametric diffeomorphic image registration with the demons algorithm. In: Ayache, N., Ourselin, S., Maeder, A.J. (eds.) MICCAI 2007, Part II. LNCS, vol. 4792, pp. 319–326. Springer, Heidelberg (2007); PMID: 18044584
8. Sermesant, M., Moireau, P., Camara, O., Sainte-Marie, J., Andriantsimiavona, R., Cimrman, R., Hill, D.L., Chapelle, D., Razavi, R.: Cardiac function estimation from MRI using a heart model and data assimilation: Advances and difficulties. Medical Image Analysis 10(4), 642–656 (2006)
9. Cawley, G.C., Talbot, N.L.C.: Fast exact leave-one-out cross-validation of sparse least-squares support vector machines. Neural Networks 17(10), 1467–1475 (2004)